web of semantic
Journal of Interdisciplinary Science | ISSN: 2960-9550
Research Article Peer-review, Open Access

Stable Isotope Analysis of Groundwater Recharge Sources and Mixing Processes on Mount Cameroon's Southern Flank

Wotany Engome Regina[1], Kuh Annubrine Loe[2], Ngai N Jude[3], Ayuk Valery Takang[4], Mbalang Betrand Kimbi[5], Mbu God Promise[6]*

Abstract

Stable isotope ($\delta^{18}O$, δD) and hydrochemical analyses were integrated to investigate groundwater recharge sources and sustainability in the volcanic aquifer along Mount Cameroon's southern flank. This region, characterized by high population density and extensive agro-industrial activities, faces escalating pressure on its groundwater resources due to climate change and anthropogenic impacts. The study examined 30 groundwater sources, and 14 monthly precipitation samples collected between December 2022 and November 2023. Results indicate that groundwater is primarily of meteoric origin, with isotopic compositions clustering near the Global Meteoric Water Line (GMWL), suggesting minimal evaporation effects. Precipitation $\delta^{18}O$ values ranged from -6.11‰ to -0.99‰, with a weighted mean of -3.22‰, while groundwater $\delta^{18}O$ ranged from -6.83‰ to -2.71‰, with a mean of -4.72. Elevated deuterium excess (d-excess: 13.18–15.60‰) further delineates dual recharge contributions from direct Atlantic precipitation and recycled continental moisture, while the absence of altitudinal $\delta^{18}O$ trends (160–961 m) confirms efficient hydrological mixing across the aquifer system. Groundwater temperatures closely mirrored ambient air temperatures, suggesting rapid recharge and shallow circulation within the aquifer. These findings provide a crucial baseline for the sustainable management of groundwater resources in this vulnerable volcanic environment, emphasizing the need for climate-resilient water policies and protection of recharge areas.

Keywords: Groundwater recharge, Stable isotopes, Deuterium excess, Volcanic aquifers, Mount Cameroon.

[1,2,3,4,5,6] Department of Geology, Faculty of Science, University of Buea, P.O. Box 63, Buea, Cameroon
[3] Institute of Geological and Mining Research, P.O. Box 4110, Yaoundé, Cameroon

1. INTRODUCTION

1.1. Background of the Study

Groundwater remains a cornerstone of global freshwater supply, sustaining critical sectors such as drinking water provision, agriculture, and industrial development (Clark & Fritz, 1997; Winter et al., 1998;Ngai et al., 2024; Muka et al., 2025; Takang et al., 2025). Nowhere is this reliance more pronounced than in Sub-Saharan Africa, where surface water scarcity, exacerbated by seasonal variability, has driven a surge in groundwater dependency amidst rapid urbanization and population growth (Bonsor et al., 2011; Fantong et al., 2016; Nyika & Dinka,2023). The southeastern flanks of Mount Cameroon vividly illustrate this trend, serving as a vital water source for expanding communities such as Buea and Mutengene.

In these areas, groundwater supplies over 60% of domestic and agro-industrial needs, underpinning water bottling operations and the irrigation of export-oriented crops such as bananas, oil palm, and pineapples (Ako et al., 2012; Akoachere et al., 2019).

Understanding the recharge dynamics of volcanic aquifers is essential for developing accurate hydrological models and sustainable water management strategies, particularly in tropical high-relief settings such as Mount Cameroon. While previous studies in the region have provided important insights into groundwater quality and general hydrochemical patterns (Wotany et al., 2013; Akoachere et al., 2019; Ngwese et al.,2025), the underlying recharge mechanisms remain poorly constrained. In particular, there has been a lack of systematic application of stable isotopes, $\delta^{18}O$, δD, and deuterium excess (d-excess), which are well-established tools for identifying recharge sources, tracing moisture pathways, and assessing the extent of evaporation and mixing in groundwater systems (Gonfiantini, 1993; Jasechko, 2019).

The absence of a region-specific Local Meteoric Water Line (LMWL) further limits the ability to interpret isotopic compositions of groundwater in terms of precipitation origin and recharge altitude. This gap is significant, as recent isotopic studies in similar humid tropical and volcanic settings have demonstrated that both Atlantic-derived and recycled continental moisture contribute variably to recharge, and that such dual-source signals are often captured in d-excess values (Natali et al., 2022; Emvoutou et al., 2024). Moreover, despite the pronounced topographic gradient on the southern flank of Mount Cameroon (160–961 m), no systematic assessment of altitude-dependent isotopic variation has been undertaken. As a result, key questions regarding vertical and lateral hydrological mixing, recharge elevation, and the role of structural controls remain unanswered.

To address these deficiencies, this study applies an integrated hydrochemical and isotopic approach to characterize the recharge regime of volcanic aquifers on the southern flank of Mount Cameroon. The primary objectives were to: (1) establish a Local Meteoric Water Line for the Buea–Mutengene catchment based on multi-seasonal precipitation data; (2) identify dominant atmospheric moisture sources contributing to recharge using $\delta^{18}O$, δD, and d-excess; (3) evaluate isotopic variation with elevation to assess the extent of hydrological mixing and vertical connectivity.

2. Location of study area.

The study area is located in the South West region of Cameroon along the Southeastern flanks of Mount Cameroon at an elevation of 160 - 961m above mean sea level. It has a surface area of about 870km^2 approximately. It is located between latitudes 9°14’0’’E to 9°20’0’’E and longitude 4°4’0’’N to 4°11’0’’N (Fig. 1).

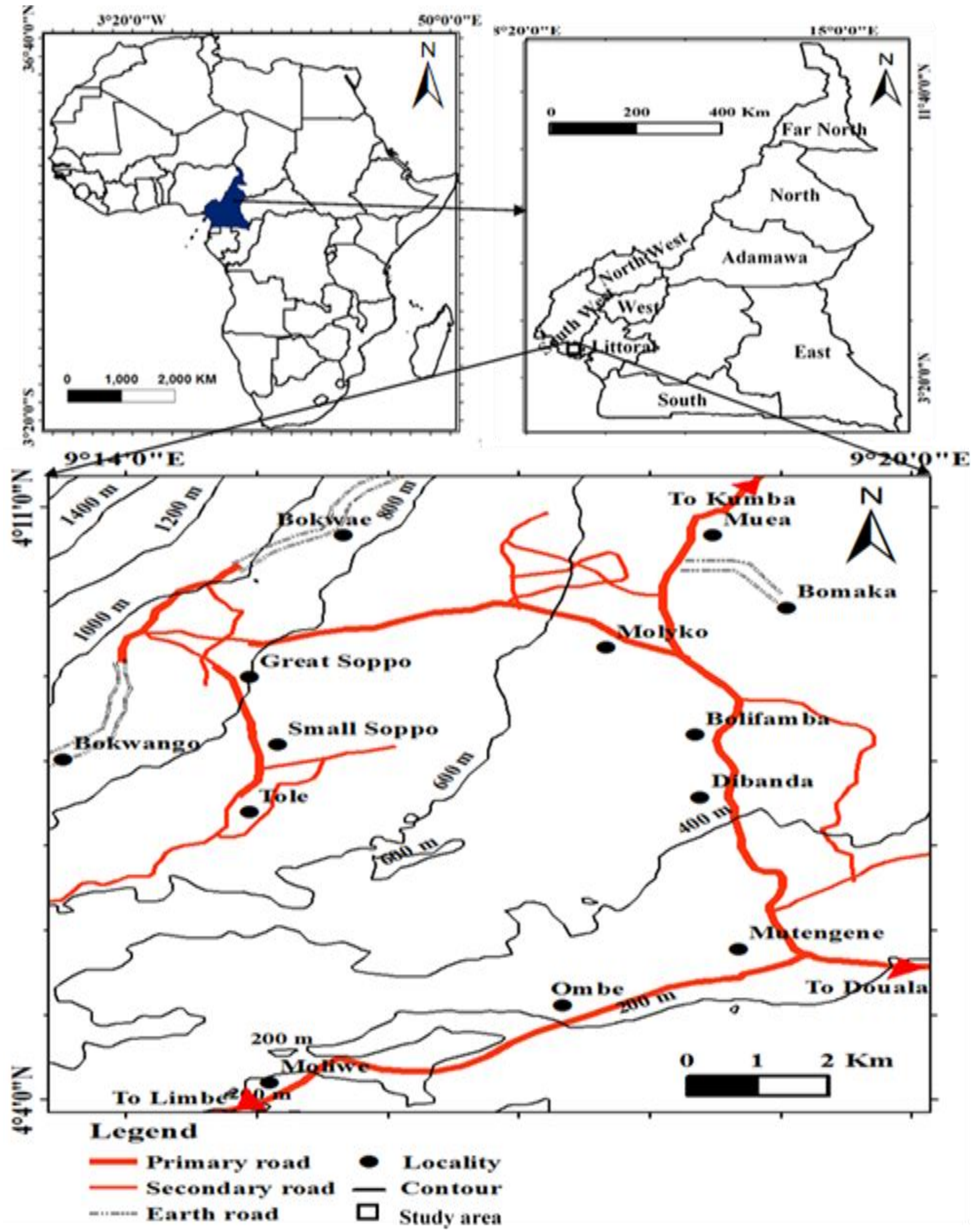

Figure 1. Location map of the study area

2.1. Biophysical Characteristics

The Fako Division's biophysical environment comprises interdependent climatic, hydrological, vegetative, and edaphic factors. Key characteristics include:

2.1.1. Climate

Subequatorial regime with a >4-month dry season (November–mid-March) and a 7-month rainy season (mid-March–October). Mean annual rainfall is ~3,100 mm ±1,100 (range: 1,500–6,000 mm), peaking June–September. Temperatures average 26°C with minimal annual variation (±4°C) (Hall et al., 1973; Ako et al., 2012; Ngai et al.,2023).

2.1.2. Drainage/Topography

Hilly terrain with high humidity and dense spring/stream networks (Fig 2). Volcanic tectonics create extensive fractures and faults in piedmont zones, forming interconnected groundwater channels that emerge as springs (Akoachere et al., 2019; Somers & McKenzie,2020).

2.1.3. Vegetation

Features West/Central Africa's only unbroken altitudinal gradient from lowland rainforest at sea level to montane forest, grassland, and alpine grassland near the summit. Primary forests at lower elevations are largely replaced by banana, palm, rubber plantations, and settlements (Hall, 1973; Couvreur et al.,2021).

2.1.4. Soils/Land Use

Dominated by volcanic ash-derived andisols, with soil organic matter increasing with altitude due to cooler temperatures. The zone is intensively farmed for banana, oil palm, rubber, pawpaw, tomatoes, watermelon, and pineapple (Ako et al., 2012, Ngai et al., 2024).

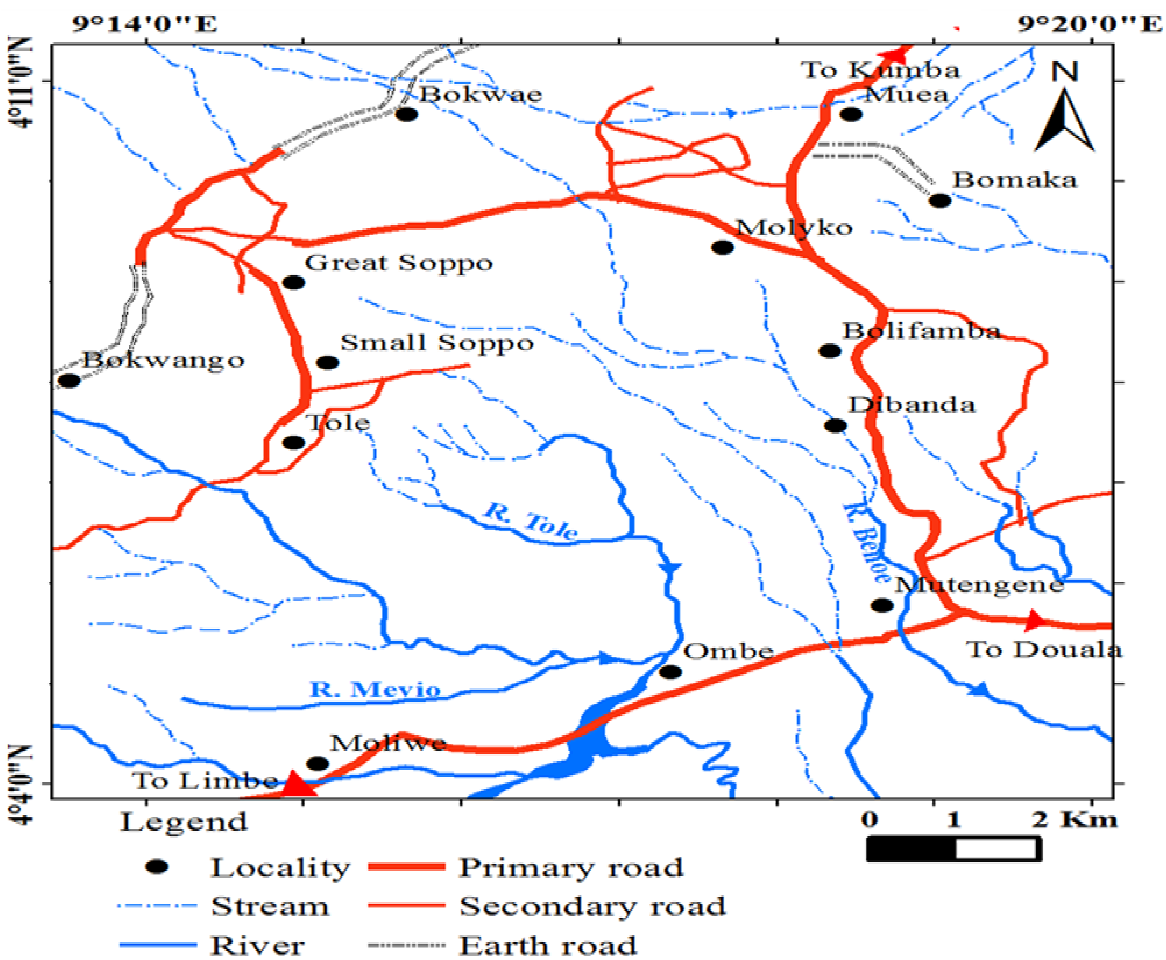

Figure 2. Drainage map showing dendritic pattern

2.2. Geology

Mount Cameroon, an active stratovolcano, represents the most prominent edifice along the Cameroon Volcanic Line (CVL), a 1,600 km long volcanic and tectonic structure extending from the Gulf of Guinea into the Central African continent (Hermann, 2023). The geology of the southern flank of Mount Cameroon is a complex integration of volcanic, tectonic, and hydrogeological systems, shaped by both deep Earth processes and intense tropical weathering (Chendjou et al., 2024) (Fig.3). This region lies atop a Precambrian crystalline basement composed primarily of gneisses, schists, and migmatites of Pan-African age (~550 Ma), which form the structural foundation of the broader South Cameroon Plateau (Ngwa et al., 2019; Azefack Mbounou et al., 2023). The volcanic rocks consist of Cenozoic lavas, predominantly basanites and hawaiites derived from mantle metasomatism and magmatic differentiation processes along the CVL (Asaah et al., 2021). These volcanic rocks are heavily weathered under tropical conditions, producing a thick regolith layer that significantly influences groundwater storage and flow. The study area is particularly characterized by the presence of numerous strombolian scoria cones and extensive basaltic lava flows, results of historic flank eruptions (Ngwa et al., 2019). These lavas exhibit geochemical signatures indicative of fractional crystallization, magma mixing, and open-system recharge processes, with evidence pointing to magma chamber activity at depths between 23 and 29 km (Brenna et al., 2021). Structurally, the region is dissected by several prominent fault systems and lineaments, predominantly trending NE–SW and N–S, which exert strong control over groundwater movement and storage (Elshalkany et al., 2025). These structural features, often acting as conduits or barriers, facilitate deep percolation of rainwater and lateral groundwater flow within the basaltic and fractured crystalline units (Akoachere et al., 2019).

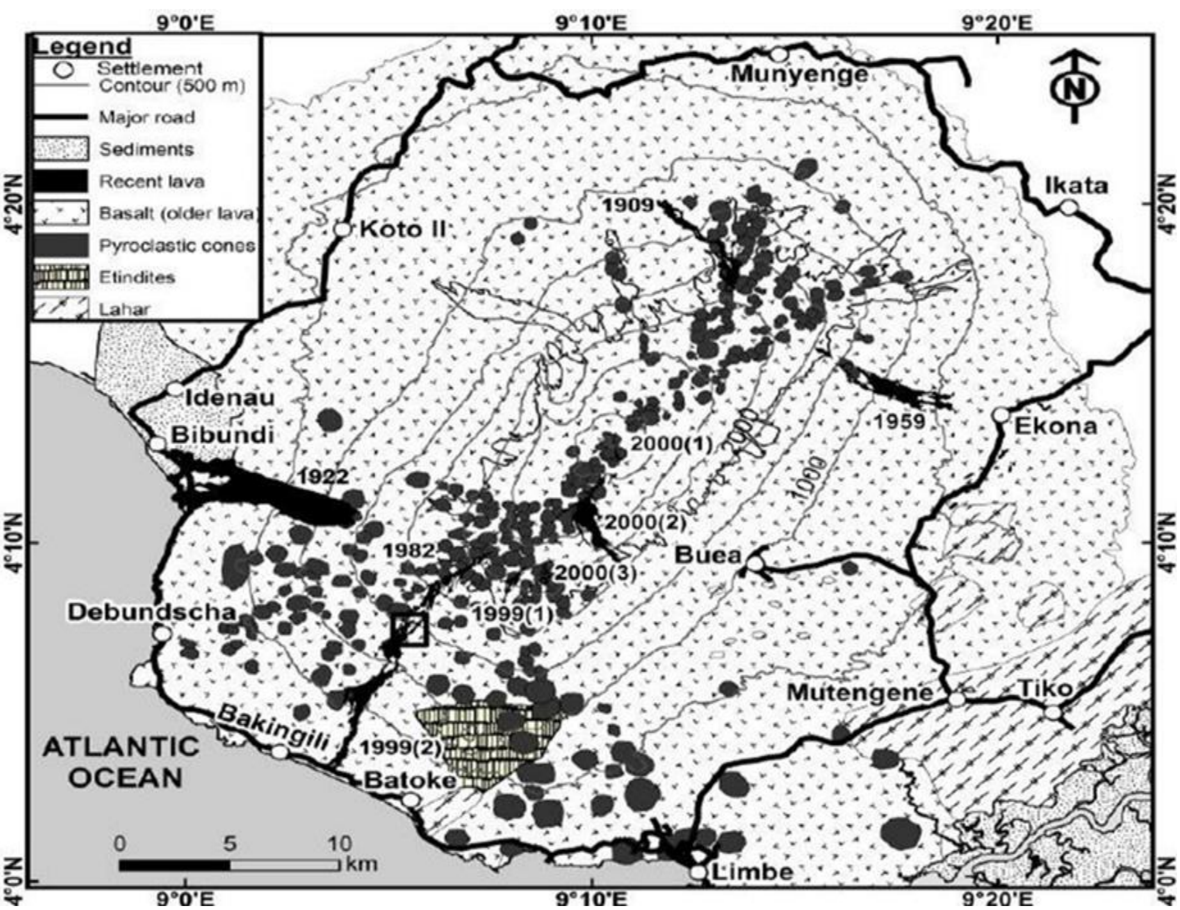

Figure. 3. Geology of the study area showing rock types (Adapted from Wantim et al., 2013)

2.3. Hydrogeology

The Mount Cameroon region sustains abundant groundwater resources due to high annual precipitation (>3,000 mm) recharging permeable volcanic formations. Pyroclastic cones overlie impermeable basaltic layers, facilitating perched aquifers as infiltrating water percolates through scoriaceous materials. The hydrogeological system is characterized by high porosity and permeability, resulting from:

1. **Fracture networks**: Extensive joints and faults in basaltic lava flows, formed by volcanic tectonics, create interconnected subsurface channels.
2. **Pyroclastic porosity**: Unwelded scoria deposits exhibit high primary porosity and water-holding capacity.
   These features enable significant groundwater storage within piedmont regions, where fractures retain large volumes of water that discharge downslope as major springs (Ako et al., 2012; Akoachere et al., 2019; Ngai et al.,2024)

3. Materials and Methods

A reconnaissance survey was conducted across the southeastern flanks of Mount Cameroon (latitudes 9°14'0"E–9°20'0"E; longitudes 4°4'0"N–4°11'0" N) to map aquifer access points. Thirty groundwater sources, 18 boreholes, 8 springs, and 4 wells were selected to represent hydrological diversity and anthropogenic exposure (proximity to agricultural/urban zones). Sampling occurred during the dry season to minimize rainfall dilution effects. Before sampling, wells and boreholes were purged for 10 minutes to eliminate stagnant water. In-situ parameters pH, electrical conductivity (EC), temperature, and total dissolved solids (TDS) were measured using a calibrated Hanna HI991300 multiprobe (±0.01 accuracy). Static water levels (Table 1) and GPS coordinates were recorded to produce the sample location map (Fig. 4).

Table 1. Results of Static water levels of groundwater samples

SN	COORDINATES (UTM)			Location Name	Sample ID	water source	Depth (m)
	LON	LAT	Elevation (m)				
1	525089	457043	937	Bokwaongo monangai	BH01	Borehole	17
2	525269	457688	961	Bokwaongo junction	BH02		20
3	531264	459557	624	Copenhager check point	BH03		19
4	531148	459829	930	Omnisport check point	BH04		25
5	531070	461200	630	Koke	BH05		30
6	530830	461244	659	koke catchment	SP01	Spring	0
7	532982	458376	531	Mile 17 New layout	BH06		20
8	533172	458386	517	Mile 17 New layout	SP02		0
9	533308	458048	514	Kombo catchment	SP03		0
10	533405	458265	517	Bulu blind	BH07		30
11	533690	458448	512	Mile 17 path finder	BH08		22
12	533363	458983	540	Chief street Bomaka	BH09		26
13	532072	459591	589	Green court Malingo	BH10		17
14	526914	457490	820	Small Soppo Wovilla	SP04		0
15	526935	458864	859	Clerks quarter Capitol	BH11		20
16	527322	459130	630	Musole Cam-water	SP05		0
17	527904	459927	835	Quarter 13 Great Soppo	BH12		18
18	529542	458065	669	Sandpit Bulu	SP06		30
19	535275	452957	262	New layout Mutengene	BH13		28
20	535646	452132	230	Quarter 8 Mutengene	OW01	Well	3.7

21	535740	451451	196	Quarter 7 Mutengene	OW02		11
22	535586	451363	189	Quarter 6 Mutengene	BH14		24
23	535310	451424	187	Quarter 5 Mutengene	OW03		4.1
24	534933	451492	192	Quarter 2 Mutengene	SP07		0
25	534263	451579	186	Bwinga Mutengene	BH15		30
26	534357	450969	160	Mango beach Mutengene	OW04		4.2
27	534735	452102	235	Quarter 18 Mutengene	BH16		29
28	530326	459333	642	Chief owusi Biaka	SP08		0
29	533192	461051	570	Quarter 6 Muea	BH17		25
30	531707	459144	591	Untarred Malingo	BH18		27

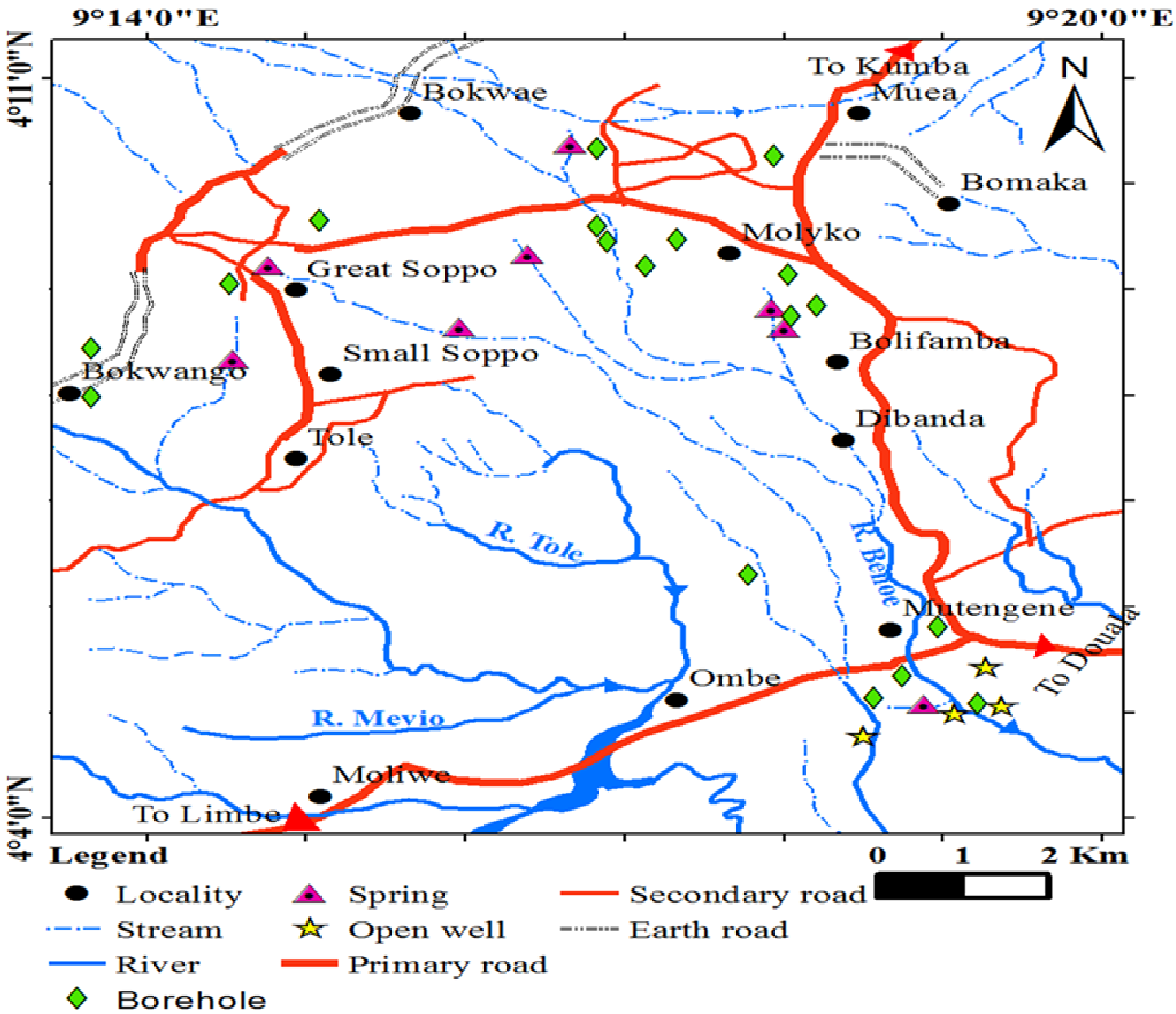

Figure 4. Sample location Map of the study area

Stable isotopes ($\delta^{18}O$, δD) were analysed at the Meteorological Research Institute (Japan) using a Picarro L2140-i cavity ring-down spectrometer. Results are reported in ‰ relative to VSMOW, with precisions of ±0.1‰ for $\delta^{18}O$ and ±0.5‰ for δD. Deuterium excess (d-excess = $\delta D - 8\delta^{18}O$) was computed to trace moisture sources.

Precipitation samples were collected as described by Goni (2006) for a period of 14 months using the Palmer rain gauge. Rain samples collected daily for 14 months were poured into 5 L sealed plastic containers. The integrated rain samples were poured into 100 mL polythene bottles, tightly capped and stored in a cold environment preceding laboratory analysis. Temperature and relative humidity measurements were also recorded. Thirty water samples obtained from ground and surface water were also put in plastic bottles (100 mL) for oxygen and hydrogen isotope analysis. The deuterium (D) and oxygen-18 (18O) compositions were analysed using a cavity ring-down spectrometer analyser (model L2120-i from Picarro), as described in Wotany et al. (2021). Total analytical precisions were ± 0.05‰ ($\delta^{18}O$) and ± 0.12‰ (δD). The precipitation weighted average values (w.a.v) of $\delta^{18}O$ and δD for each month and the annual values were computed from Eq. 1(IAEA 1992):

$$\sum_{1}^{n} Pi\delta / \sum_{1}^{n} Pi \qquad (1)$$

where P_i is rainfall amount, and δ_i is isotopic composition per month. The deuterium-excess (*d*-excess) parameter was obtained as defined by Dansgaard (1964) as:

$$d=\delta D-8\delta 18O \qquad (2)$$

4. Results

Groundwater samples exhibited acidic to basic pH range (6.6–8.2; mean 7.35), with the highest value at Koke Spring and the lowest at Mile 17 Borehole and Mutengene wells. Electrical conductivity (EC) ranged from 140–570 µS/cm (mean 286.33 µS/cm), peaking at Quarter 2 Spring (Mutengene) and reaching minima at Quarter 6 Muea and Quarter 13 Soppo boreholes. Total dissolved solids (TDS) averaged 140 mg/L (70–280 mg/L), highest at Quarter 2 Spring (Mutengene) and lowest at Bokwaongo, Great Soppo, Muea, and Musole Camwater sources. The temperature averaged 26.26°C (23–29°C).

Table 2. Statistical summary of physicochemical parameters of 30 groundwater samples.

Location	ID	Temp	pH	EC	TDS
Bokwaongo Monangai	BH01	26.00	7.60	270.00	130.00
Bokwaongo junction	BH02	24.00	7.70	160.00	70.00
Copenhager check point	BH03	26.00	7.40	250.00	120.00
Omnisport stadium check point	BH04	26.00	7.60	210.00	100.00
Koke	BH05	28.00	7.70	220.00	110.00
koke catchment	SP01	24.00	8.20	240.00	120.00
Mile 17 New layout	BH06	27.00	6.60	300.00	150.00
Mile 17 New layout	SP02	25.00	7.60	270.00	130.00
Kombo catchment	SP03	24.00	7.00	230.00	110.00
Bulu blind	BH07	26.00	7.80	280.00	130.00
Mile 17 path finder	BH08	27.00	7.10	230.00	110.00
Chief street Bomaka	BH09	25.00	7.10	280.00	140.00
Green court Malingo	BH10	24.00	7.10	370.00	180.00
Small Soppo Wovilla	SP04	23.00	7.60	200.00	100.00
Clerks quarter Capitol	BH11	25.00	7.60	340.00	170.00
Musole Cam-water	SP05	24.00	8.20	150.00	70.00
Quarter 13 Great Soppo	BH12	25.00	7.40	140.00	70.00
Sandpit Bulu	SP06	27.00	7.30	250.00	130.00
New layout Mutengene	BH13	28.00	7.30	230.00	110.00
Quarter 8 Mutengene	OW01	28.00	6.60	390.00	190.00
Quarter 7 Mutengene	OW02	29.00	6.60	370.00	180.00
Quarter 6 Mutengene	BH14	28.00	7.40	500.00	250.00
Quarter 5 Mutengene	OW03	29.00	6.60	530.00	260.00
Quarter 2 Mutengene	SP07	29.00	7.40	570.00	280.00

Bwinga Mutengene	BH15	28.00	7.80	330.00	160.00
Mango beach Mutengene	OW04	28.00	7.30	300.00	150.00
Quarter 18 Mutengene	BH16	29.00	7.30	360.00	170.00
Chief owusi street Biaka	SP08	23.00	7.80	220.00	110.00
Quarter 6 Muea	BH17	27.00	6.80	140.00	70.00
Untarred Malingo	BH18	26.00	6.90	260.00	130.00
Minimum		23.00	6.60	140.00	70.00
Maximum		29.00	8.20	570.00	280.00
Mean		26.27	7.35	286.33	140.00
SD		1.89	0.44	107.62	53.43
WHO (2018) standard		30.00	6.5-8.5	750.00	500.00

The stable isotope analysis of 30 groundwater and surface water samples (Table 3) reveals $\delta^{18}O$ values ranging from -3.10‰ to -5.21‰ (mean ≈ -4.1‰) and δD values from -10.99‰ to -27.01‰ (mean ≈ -18.5‰). Notably, d-excess values are consistently elevated (13.18‰–15.60‰), exceeding the global average of 10‰. This high d-excess indicates that groundwater recharge occurs under conditions of minimal evaporation, likely through rapid infiltration of precipitation into the aquifer system.

Table 3. Stable isotope composition of 30 groundwater samples.

S/N	Location	Sample ID	Alt (m)	$\delta^{18}O$ ‰	δD‰	d-excess‰
1	Bokwaongo monangai	BH01	937	-4.09	-19.26	13.50
2	Bokwaongo junction	BH02	961	-4.06	-18.08	14.39
3	Copenhager check point	BH03	624	-4.17	-19.08	14.26
4	Omnisport check point	BH04	930	-3.65	-15.52	13.66
5	Koke	BH05	630	-4.57	-21.66	14.86
6	koke catchment	SP01	659	-4.98	-24.21	15.60
7	Mile 17 New layout	BH06	531	-4.21	-19.46	14.22
8	Mile 17 New layout	SP02	517	-4.33	-20.11	14.55
9	Kombo catchment	SP03	514	-4.23	-19.43	14.38
10	Bulu blind	BH07	517	-4.80	-23.30	15.10
11	Mile 17 path finder	BH08	512	-3.30	-13.01	13.42
12	Chief street Bomaka	BH09	540	-4.82	-23.71	14.83
13	Green court Malingo	BH10	589	-3.75	-15.85	14.11
14	Small Soppo Wovilla	SP04	820	-4.64	-21.97	15.14
15	Clerks quarter Capitol	BH11	859	-5.10	-26.04	14.78
16	Musole Cam-water	SP05	630	-4.51	-21.32	14.77
17	Quarter 13 Great Soppo	BH12	835	-4.44	-21.25	14.31
18	Sandpit Bulu Catchment	SP06	669	-5.21	-27.01	14.70
19	New layout Mutengene	BH13	262	-3.28	-10.99	15.21
20	Quarter 8 Mutengene	OW01	230	-3.91	-17.66	13.59
21	Quarter 7 Mutengene	OW02	196	-3.34	-13.12	13.60
22	Quarter 6 Mutengene	BH14	189	-3.57	-13.06	15.48
23	Quarter 5 Mutengene	OW03	187	-3.10	-11.26	13.57
24	Quarter 2 Mutengene	SP07	192	-3.43	-12.75	14.65
25	Bwinga Mutengene	BH15	186	-3.44	-12.47	15.08
26	Mango beach Mutengene	OW04	160	-3.40	-12.05	15.19
27	Quarter 18 Mutengene	BH16	235	-3.30	-12.42	13.96
28	Chief owusi street Biaka	SP08	642	-4.48	-20.72	15.12
29	Quarter 6 Muea	BH17	570	-3.35	-13.62	13.18

30	Untarred Malingo	BH18	591	-4.13	-18.25	14.76

Table 4: Summary of rain water result

Month	δ^{18} O (‰)	δD (‰)	d-excess (‰))	Rainfall (mm)
July	-4.27	-20.70	13.46	323.65
August	-2.07	-3.90	12.66	465.1
September	-5.11	-32.90	7.98	409.21
October	0.43	8.40	4.96	306.04
November	-4.37	-24.70	10.26	104.54
January			0	17.82
February	1.73	7.40	-6.44	38.19
March	-3.18	-12.40	13.04	142.99
April	-3.63	-19.70	9.34	198.14
May			0	234.55
June	-3.74	-14.50	15.42	324.62
July	-3.72	-14.40	15.36	323.65
August	-5.42	-32.60	10.76	465.1
September	-5.46	-32.90	10.78	409.21
October	-5.45	-32.80	10.8	306.04
November	-3.34	-15.60	11.12	104.54
December			0	22.95

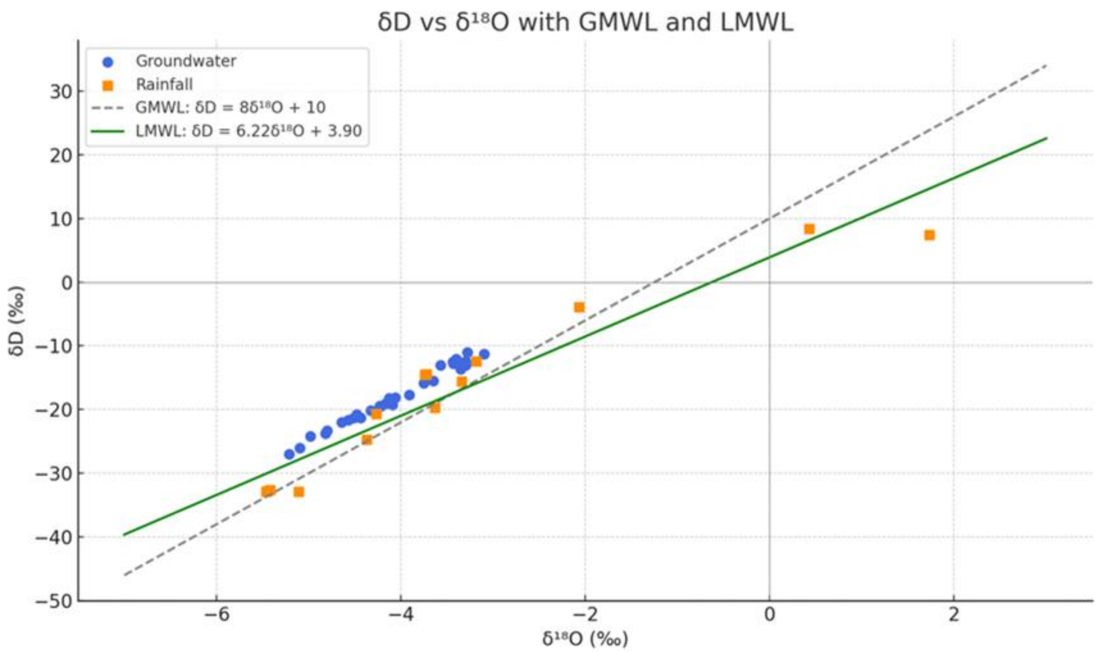

Figure 5. Plot of δ^{18}O versus δD relationship of rainfall, ground and surface water in the study area

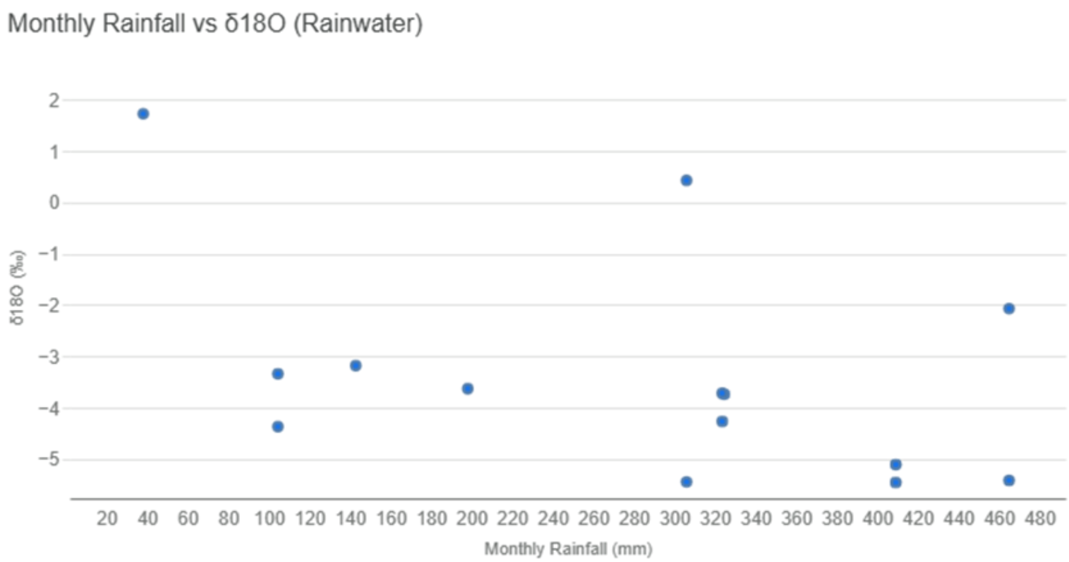

Figure 6: Inverse relationship between monthly rainfall amounts and weighted mean of δ18O

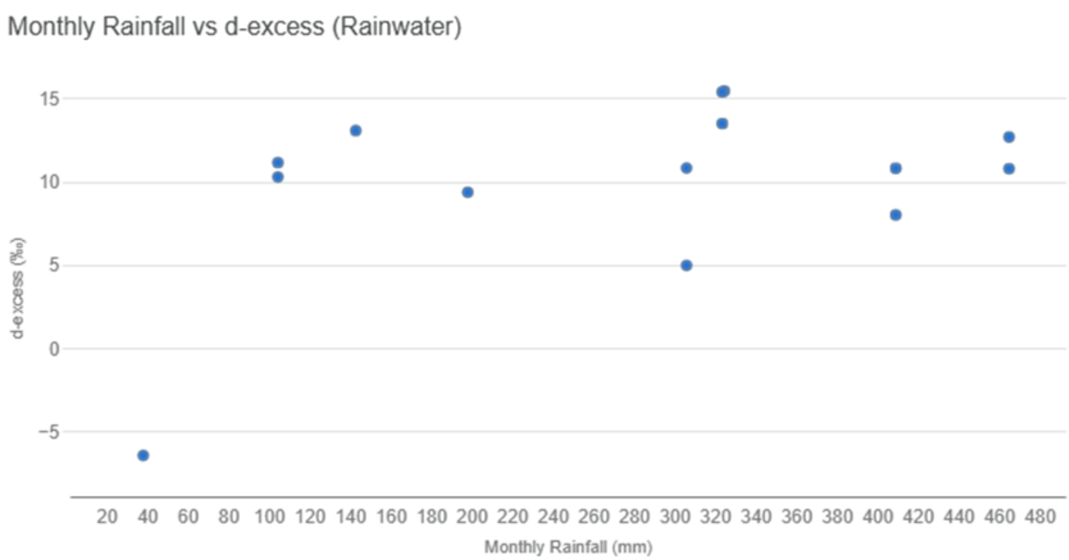

Figure 7: Inverse relationship between monthly rainfall amounts and d-excess

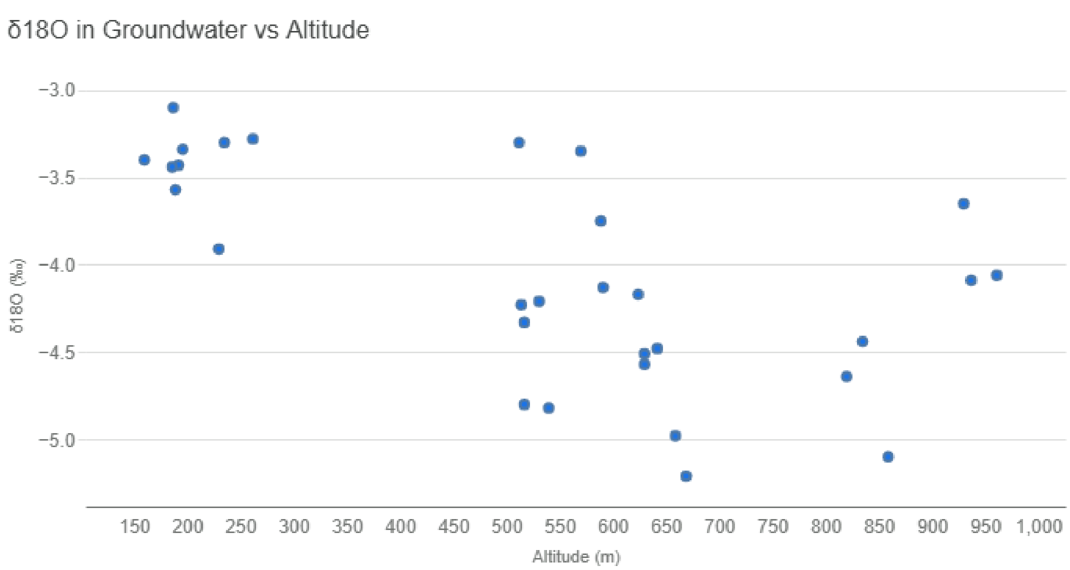

Figure 8. Plot of δ18O in ground and surface water as a function of altitude

The alignment of all samples near the Global Meteoric Water Line (GMWL) in Fig. 5 further confirms their meteoric origin, ruling out significant evaporation or mixing with other water sources (Terzer-Wassmuth et al.,2023).

Rainwater isotope data (Table 4) exhibit strong seasonal contrasts: wet-season months (September: $\delta^{18}O$ = -5.46‰) show notably depleted isotopes compared to dry periods (February: $\delta^{18}O$ = +1.73‰). Crucially, Figs. 6 and 7 demonstrate an inverse relationship between monthly rainfall amount and isotopic composition**,** higher rainfall correlates with more depleted $\delta^{18}O$ and lower d-excess. This suggests wet-season rainfall originates from distilled oceanic moisture with secondary evaporation during convection, while dry-season precipitation reflects local moisture recycling or continental air masses (higher d-excess).

Despite sampling elevations from 160–961 m, no systematic trend emerges (high-altitude BH15: -5.10‰ vs. low-altitude BH15: -3.44‰). This implies hydrological mixing across elevations, likely through interconnected flow paths or dominant recharge in topographically similar zones. The groundwater's homogeneous d-excess contrasts with rainwater's seasonal variability, indicating aquifer recharge integrates precipitation across multiple seasons, resulting in a stable isotopic signature.

The results characterize a system where groundwater is predominantly recharged by local rainfall with minimal evaporative loss. The pronounced amount effect in rainfall reflects tropical hydroclimate dynamics, while the lack of altitude dependence and uniform d-excess in groundwater point to well-mixed aquifers with efficient recharge mechanisms. These patterns collectively suggest resilient groundwater resources buffered against seasonal precipitation variability in the study area.

Fig. 9 shows a plot of Cl^-, TDS and $\delta^{18}O$ which shows a lack of correlation between TDS and $\delta^{18}O$. An increase in chloride is observed without a corresponding increase in $\delta^{18}O$ composition.

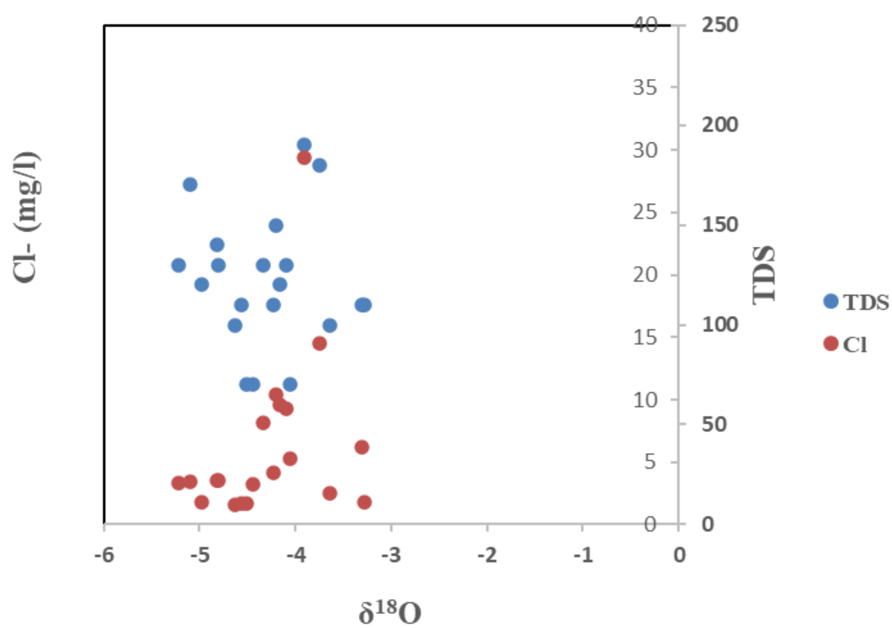

Figure 9. A cross plot of $\delta^{18}O$ against TDS and Cl^- showing inverse relationship between $\delta^{18}O$ against TDS and Cl^-.

4. Discussion

4.1. Aquifer Characteristics

Groundwater temperatures (mean 26.3°C) align closely with mean annual air temperature (26°C), indicating shallow phreatic aquifers (<10 m depth) with rapid modern recharge driven by present-day climate (Wirmvem et al., 2017; Akoachere et al., 2019; Fenta,2022). This thermal equilibrium mirrors young volcanic aquifers in Hawaii (Scholl et al., 1996) but contrasts with deep, thermally buffered systems like the Nubian Sandstone Aquifer (Sturchio et al., 2004; Ferguson, 2020). The acidic-basic pH (6.6–8.2) reflects bicarbonate dissolution (HCO_3-dominant) and basaltic weathering (Ako et al., 2012; Day & Marquez, 2023), diverging from acidic conditions in sulfide-rich regions (Sánchez-Martínez et al., 2012; Ludyan,2020). Low EC (140–570 µS/cm) and TDS (70–280 mg/L) confirm mineral-poor fresh groundwater (Todd, 2005; Bayram,2023), akin to silicate aquifers in the Deccan Traps (Gupta et al., 2011; Saiers et al.,2021) but distinct from evaporite-influenced waters in the Jordan Rift (Abu-Rukah & Ghrefat, 2004).

4.2. Isotopic Characterization of Recharge Mechanisms

The tight clustering of $\delta^{18}O$ (−5.21‰ to −3.10‰) and δD (−27.01‰ to −10.99‰) along both the Global Meteoric Water Line (GMWL: $\delta D = 8\delta^{18}O + 10$; Craig, 1961) and the Local Meteoric Water Line (LMWL: $\delta D = 7.36\delta^{18}O + 11.71$; Fantong et al., 2010, Nlend et al., 2023) confirms a meteoric origin and rapid infiltration of recharge waters, with minimal evaporative enrichment. This recharge dynamic is consistent with observations in Réunion Island basalts (Join et al., 2025) but markedly contrasts with the evaporated groundwater profiles of the Sahel (Fontes et al., 1993; Belle et al.,2018). High deuterium excess values (d-excess: 13.18–15.60‰) surpass the Atlantic baseline (~10‰), indicating a dual-origin recharge mechanism: primary input from Atlantic monsoon precipitation (Rozanski et al., 1993; Torres-Martínez et al.,2020; Isson & Rauzi,2024) and secondary contributions from rainforest-derived recycled moisture (d-excess > 14‰; Dansgaard, 1964; Wotany et al., 2021). This isotopic signature mirrors hydrological patterns in the Amazon Basin (Gat & Matsui, 1991; Natali et al.,2022) and exceeds the relatively lower d-excess values reported for the Ganges Basin (Deshpande et al., 2003; Mao et al 2021; Qu et al.,2024), underscoring the influence of complex atmospheric moisture recycling in the region.

4.3. Hydrological Mixing and Salinity Drivers

The absence of a correlation between $\delta^{18}O$ and elevation across the 160–961 m range suggests vertical isotopic homogenization driven by fracture connectivity, effectively overriding the expected altitude effect on isotopic depletion observed in mountainous settings like the Andes (Gonfiantini et al., 2001; Vystavna et al.,2021). This pattern aligns with findings from the Azores Islands, where Cruz and Amaral (2004) and Andrade et al. (2024) attributed isotopic uniformity to cross-elevation mixing via volcanic fracture networks, in contrast to stratified flow systems seen in the Alpine region (Bershaw et al., 2012; Zhu et al.,2023). Additionally, the lack of $\delta^{18}O$–TDS correlation ($R^2 < 0.2$) coupled with chloride enrichment up to 45 mg/L, without accompanying isotopic enrichment, rules out evaporative concentration as the salinity source, unlike the evaporated groundwater signatures documented in Australian playas (Herczeg et al., 2001; Zhang et al.,2025). Conversely, the data suggest geogenic salinity input via weathering of chloride-bearing lithologies, such as amphiboles, consistent with observations in Saka et al. (2013) and tectonically active rift settings like the East African Rift (Rango et al., 2010; Burnside et al.,2021).

4.4. Recharge Model Synthesis and Climate Resilience

The isotopic dataset supports a dual-origin piston-flow recharge model, comprising focused infiltration of Atlantic-sourced precipitation through fractures occurring over short timescales (Njitchoua et al., 1999; Jasechko,2019), coupled with diffuse recharge from forest-derived recycled moisture characterized by elevated d-excess values (Gat & Matsui, 1991; Pederzani & Britton,2019). The narrow $\delta^{18}O$ range eliminates the influence of paleowaters, confirming the dominance of modern recharge processes (Fontes & Olivry, 1977; Wotany et al.,2021; Emvoutou et al.,2024), in contrast to the presence of Pleistocene signatures in deeper Saharan aquifers (Guendouz et al., 2003; Eid et al.,2024). Furthermore, the stable isotope consistency during prolonged dry seasons (>4 months) underscores the aquifer system's resilience and suggests steady flow dynamics akin to those observed in high-altitude Andean páramos (Buytaert et al., 2006; Somers & McKenzie,2020).

4.5. Global Context and Management Implications

The aquifer system demonstrates both vulnerability and resilience: its rapid recharge via fractured pathways enhances the risk of contamination, particularly from nitrate pollution in urbanized catchments, as observed by Ako et al. (2014) and Mielby & Henriksen,(2020). and corroborated by recent findings in Nairobi's expanding peri-urban zones (Olago et al., 2023). Nevertheless, the dual-source recharge combining Atlantic monsoonal input and rainforest-recycled moisture bolsters its resilience against seasonal and long-term drought, a trait superior to that of single-source recharge systems such as those in the hyper-arid Atacama Desert (Houston, 2006; Halkes et al.,2024). To ensure long-term sustainability, it is imperative to protect key recharge areas, especially the forested highlands and structurally controlled infiltration zones, in line with recharge conservation strategies implemented around Mt. Kenya (Olago, 2001). Simultaneously, monitoring geogenic risks such as fluoride and bromide release, as practiced in the Ethiopian Rift system (Rango et al., 2010; Bianchini et al.,2020), should be prioritized to mitigate chronic exposure hazards in vulnerable lowland communities.

5. Conclusion

The integration of physicochemical parameters and stable isotope data provides definitive insights into the recharge characteristics of the Mount Cameroon volcanic aquifers. Groundwater exhibits acidic-basic pH conditions (6.6–8.2) and temperatures (23–29°C; mean 26.3°C) closely mirroring mean annual atmospheric temperatures (26°C), indicative of shallow, rapidly recharged systems. Critically low mineralization is evidenced by consistently fresh groundwater, with total dissolved solids (TDS: 70–280 mg/L) and electrical conductivity (EC: 140–570 µS/cm) confirming minimal solute acquisition during infiltration. Stable isotopic signatures ($\delta^{18}O$: −5.21‰ to −3.10‰; δD: −27.01‰ to −10.99‰) rigorously adhere to the Local Meteoric Water Line ($\delta D = 7.36\delta^{18}O + 11.71$; $r^2 = 0.98$), unambiguously establishing a meteoric origin without evaporative alteration. Elevated deuterium excess (d-excess: 13.18–15.60‰) further delineates dual recharge contributions from direct Atlantic precipitation and recycled continental moisture while the absence of altitudinal $\delta^{18}O$ trends (160–961 m) confirms efficient hydrological mixing across the aquifer system. The physicochemical and isotopic lines of evidence validate dominantly rapid, low-evaporation recharge mechanisms governing groundwater sustainability in this volcanic terrain.

Acknowledgement:

We would like to acknowledge the contribution of the Takeshi Ohba Laboratory, Tokai University, Japan for the isotopes analysis.

Declaration

Clinical trial number

Not applicable

Ethics approval and consent to participate

All procedures were performed in accordance with the ethical standards of the institutional committee.

Consent for publication

Not applicable

Funding declaration: No funding

Data availability: Available at any time upon request

Conflict of interest

The authors declare no conflict of interest

Authors' Contributions statement: Dr.Wotany Engome Regina, Kuh Annubrine Loh, Ngai Nfor Jude, Ayuk Valery Takang, Mbalang Betrand Kimbi, and Mbu God Promise contributed to conceptualization, methodology, formal analysis, resource allocation, and the preparation of the original draft. The authors have reviewed and sanctioned the final version of the material for publication.

REFERENCES

1. Abu-Rukah, Y., Ghrefat, H.A. (2004) Ion chemistry of waters impounded by the Ziqlab dam, Jordan, and weathering processes- a case study. International journal of Environment and Pollution, 263-276.
2. Ako, A. A., Shimada, J., Hosono, T., Ka gabu, M., Ayuk, A. R., Nkeng, G. E., Takem, G. E. E., & Takounjou, A. L. F. (2012). Spring water quality and usability in the Mount Cameroon area revealed by hydrogeochemistry. Environmental Geochemistry and Health. doi:10.1007/s10653-012-9453-3
3. Ako, A.A., Eyong, G.E.T., Shimada, J., (2014). Nitrate contamination of groundwater in two areas of the Cameroon Volcanic Line (Banana Plain and Mount Cameroon area). Appl Water Sci. 4, 99-113.
4. Akoachere, R. A., Hosono, T., Eyong, T. A., Ngassam, M.-C. P., & Oben, T. T. (2019). Assessing the Trace Metal Content of Groundwater in the Bakassi Peninsular, Onshore Rio Del Rey, Akwa-Mundemba, Cameroun. Journal of Geoscience and Environment Protection, 7, 23-48.
5. Asaah, A. N. E., Yokoyama, T., Iwamori, H., Aka, F. T., Kuritani, T., Usui, T., ... & Ohba, T. (2021). High–μ signature in lavas of Mt. Oku: Implications for lithospheric and asthenospheric contributions to the magmatism of the Cameroon Volcanic Line (West Africa). *Lithos*, *400*, 106416.
6. Azefack Mbounou, R. L., Ganno, S., Ngnotue, T., Tanko Njiosseu, E. L., Fossi, D. H., Ngassam Mbianya, G., & Ayonta Kenne, P. (2023). Structural and kinematic analysis of the Nkondjock shear zone, central Cameroon: implications on the geodynamic evolution of the Central African Fold Belt. Arabian Journal of Geosciences, 16(4), 240.
7. Bayram, A. F. (2023). Hydrogeochemistry and geothermometry of the Ilgın geothermal field, Central Turkey. *Island Arc*, *32*(1), e12478.
8. Belle, P., Aunay, B., Lachassagne, P., Ladouche, B., & Join, J. L. (2018). Control of tropical landcover and soil properties on landslides' aquifer recharge, piezometry and dynamics. *Water*, *10*(10), 1491.
9. Benedetti, M. F., Dia, A., Riotte, J., Chabaux, F., Gerald, M., Boule`gue, J., et al. (2003). Chemical weathering of basaltic lava flows undergoing extreme climatic conditions: The water geochemistry record. Chemical Geology, 201, 1–17.
10. Bianchini, G., Brombin, V., Marchina, C., Natali, C., Godebo, T. R., Rasini, A., & Salani, G. M. (2020). Origin of fluoride and arsenic in the main Ethiopian rift waters. *Minerals*, *10*(5), 453.
11. Brenna, M., Ubide, T., Nichols, A. R., Mollo, S., & Pontesilli, A. (2021). Anatomy of intraplate monogenetic alkaline basaltic magmatism: clues from magma, crystals, and glass. *Crustal Magmatic System Evolution: Anatomy, Architecture, and Physico-Chemical Processes*, 79-103.
12. Burnside, N., Montcoudiol, N., Becker, K., & Lewi, E. (2021). Geothermal energy resources in Ethiopia: Status review and insights from hydrochemistry of surface and groundwaters. *Wiley Interdisciplinary Reviews: Water*, *8*(6), e1554.
13. Chendjou, L. C. K., Kenfack, J. V., Koué, J. T., & Dongmo, A. K. (2024). Interpretation of Geological and Gravity Data from the Bamiléké Plateau (West-Cameroon): Implication for the

Understanding of Its Underground Lithotectonic Geometry. Journal of Geoscience and Environment Protection, 12(9), 283-314.

14. Clark, I. D., & Fritz, P. (1997). Environmental isotopes in hydrogeology (p. 328). New York: Lewis.
15. Couvreur, T. L., Dauby, G., Blach‐Overgaard, A., Deblauwe, V., Dessein, S., Droissart, V., ... & Sepulchre, P. (2021). Tectonics, climate and the diversification of the tropical African terrestrial flora and fauna. *Biological Reviews*, *96*(1), 16-51.
16. Craig, H., 1961a, Isotopic variations in meteoric waters. Science, 133, pp. 1702-03.
17. Dansgaard W (1964) Stable isotope in precipitation. Tellus. 16, 436 – 468
18. Day, S., & Marquez, J. E. (2023). Selenium distribution in the gossan of a porphyry copper deposit, Red Chris Mine, British Columbia, Canada. *Economic Geology*, *118*(3), 599-620.
19. Dechangue, T. R., & Kabeyene Veronique, K. (2023). Use hydrochemistry and environmental isotopes for the assessment mineralization of groundwater in Miopliocene aquifers in Douala 3 (Cameroon). *American Journal of Water Resources, 11*(1), 11–19.
20. Djeito A.E, Agyingi C.M, Manga V.E, Bukalo N.N, Beka E.T (2017) Geo-Electrical and Borehole Investigation of Groundwater in some Basalts on the South-Eastern Flank of Mount Cameroon, West Africa. Journal of water Resources and Protection.10, 9-12
21. Durov, S. A. (1948). Natural waters and graphical representation of their composition. Doklady Akademii Nauk SSSR, 59, 87–90.
22. Eid, M. H., Elbagory, M., Tamma, A. A., Gad, M., Elsayed, S., Hussein, H., ... & Péter, S. (2023). Evaluation of groundwater quality for irrigation in deep aquifers using multiple graphical and indexing approaches supported with machine learning models and GIS techniques, Souf Valley, Algeria. *Water*, *15*(1), 182.
23. Elshalkany, M., Ahmed, M., Sauck, W., Abouelmagd, A., Mansour, S., El-Nekhiely, I. N., ... & Omar, A. (2025). Geophysical and Remote-Sensing Constraints on the Fault Controls on Groundwater Accumulation in Basement Rock Aquifers in Sinai, Egypt. *Surveys in Geophysics*, *46*(3), 627-664.
24. Emvoutou, H. C., Ndomè, E. P. E., Diongue, D. M., Ndam, J. R., Stumpp, C., Ketchemen-T, B., ... & Faye, S. (2024). Hydrochemical and isotopic studies providing a new functional model for the coastal aquifers in Douala Coastal Sedimentary Basin (DCSB)/Cameroon. *Science of the Total Environment*, *912*, 169412.
25. Fantong WY (2010) Hydrogeochemical and environmental isotopic study of groundwater in Mayo Tsanaga River basin, northern Cameroon: Implication for public groundwater supply management. Ph.D Thesis, University of Toyama, p.211
26. Fantong, W.Y., Fouepe A.T., Ketchemen-Tandia B et al. (2016). Variations of hydrogeochemical characteristics of water in surface flows, shallow wells and boreholes in the coastal city of Douala (Cameroon). Hydrolog Sci J. doi: 10. 1080/02626667.2016.1173789
27. Fenta, M. C. (2022). *Hydrogeophysical and hydrogeochemical characterization of volcanic aquifers in Northwest Ethiopia* (Doctoral dissertation, Szegedi Tudomanyegyetem (Hungary)).
28. Ferguson, C. M. (2020). *Exploration for Blind Geothermal Resources in the State of Hawai'i Utilizing Dissolved Noble Gasses in Well Waters* (Master's thesis, University of Hawai'i at Manoa).
29. Fonteh, M.L., Fonkou, T., Fonteh, M.F., Njoyim, E.B.T and Lambi, C.M. (2017) Spatial variability and contamination levels of Fresh water Resources by saline Intrusion in the Coastal Low-lying Areas of the Douala Metropolis Cameroon. Journal of water Resource and Protection, 9, 215-237.

30. Fontes JC (1980) Environmental isotopes in groundwater hydrology. In: Fritz P, Fontes JC (eds) Handbook of environmental isotope geochemistry, vol 1., The terrestrial environment A. Elsevier, Amsterdam, pp 75–140
31. Fontes JC, Olivry JC (1977) Composition isotopique des précipitations de la region du Mont Cameroun. ONAREST. Inst. De Recherches sur les Techniques, l'Industrie et le Soussol. pp. 28.
32. Garg, V. K., Suthar, S., Singh, S., Sheoran, A., Garima, M., & Jain, S. (2009). Drinking water quality of southwestern Haryana India: Assessing human health risks associated with hydrochemistry. Environmental Geology, doi:10.1007/s002540081636y.
33. Gat, J. R., & Matsui, E. (1991). Atmospheric water balance in the Amazon Basin: an isotopic evapotranspiration model. *Journal of Geophysical Research: Atmospheres*, *96*(D7), 13179-13188.Gat, J. R., & Matsui, E. (1991). Atmospheric water balance in the Amazon Basin: an isotopic evapotranspiration model. *Journal of Geophysical Research: Atmospheres*, *96*(D7), 13179-13188.Gat, J. R., & Matsui, E. (1991). Atmospheric water balance in the Amazon Basin: an isotopic evapotranspiration model. *Journal of Geophysical Research: Atmospheres*, *96*(D7), 13179-13188.
34. Gibbs RJ (1970). Mechanisms controlling world water chemistry. Sc. 17: 1088-1090.
35. Gonfiantini R, Roche MA, Olivry JC, Fontes JC, Zuppi GM (2001) The altitude effecton the isotopic composition of tropical rains. Chem. Geol. 181, 147 – 167.
36. Goni, I.B. (2006) The challenge of meeting domestic water supply in Nigeria. Journal of Mining and Geology 42 (1):51-55.
37. Guendouz, A., Moulla, A. S., Edmunds, W. M., Zouari, K., Shand, P., & Mamou, A. (2003). Hydrogeochemical and isotopic evolution of water in the Complexe Terminal aquifer in the Algerian Sahara. *Hydrogeology journal*, *11*, 483-495.
38. Halkes, R. T., Hughes, A., Wall, F., Petavratzi, E., Pell, R., & Lindsay, J. J. (2024). Life cycle assessment and water use impacts of lithium production from salar deposits: Challenges and opportunities. *Resources, Conservation and Recycling*, *207*, 107554.
39. Hall, J.B. (1973) Vegetational zones on the southern slopes of Mount Cameroon. Springer, 27,49-69.
40. Hem, J. D. (1989). The study and interpretation of the chemical characteristics of natural waters (3rd ed.). US Geological Survey.
41. Hermann, J. (2023). *Evolution Of The Subcontinental Lithospheric Mantle Below A Major Tectono-Volcanic Structure: Constraints From Mantle Xenoliths Along The Cameroon Volcanic Line* (Doctoral dissertation, Department of Earth Sciences, ETH Zurich).
42. Hounslow, A. W. (1995). Water quality data: analysis and interpretation (p. 416). Boca Raton: Lewis Publishers.
43. Isson, T., & Rauzi, S. (2024). Oxygen isotope ensemble reveals Earth's seawater, temperature, and carbon cycle history. *Science*, *383*(6683), 666-670.
44. Jasechko, S. (2019). Global isotope hydrogeology―review. *Reviews of Geophysics*, *57*(3), 835-965.
45. Mao, H., Wang, G., Shi, Z., Liao, F., & Xue, Y. (2021). Spatiotemporal variation of groundwater recharge in the lower reaches of the Poyang Lake Basin, China: insights from stable hydrogen and oxygen isotopes. *Journal of Geophysical Research: Atmospheres*, *126*(6), e2020JD033760.
46. Mielby, S., & Henriksen, H. J. (2020). Hydrogeological studies integrating the climate, freshwater cycle, and catchment geography for the benefit of urban resilience and sustainability. *Water*, *12*(12), 3324.

47. Muka, B., Wotany, R. E., & Agyingi, C. M. (2025). Water quality analysis in Manoka Island and Youpwé, Douala, Cameroon: Hydrogeochemical and bacteriological perspectives.

48. Natali, S., Doveri, M., Giannecchini, R., Baneschi, I., & Zanchetta, G. (2022). Is the deuterium excess in precipitation a reliable tracer of moisture sources and water resources fate in the western Mediterranean? New insights from Apuan Alps (Italy). Journal of Hydrology, 614, 128497. https://doi.org/10.1016/j.jhydrol.2022.128497

49. Ngai Nfor Jude, Engome Regina Wotany, Christopher Agyingi, Zacharie Ekoa Armel, (2023) Hydrogeochemical characterization of groundwater quality, East of Mount Cameroon and West of the Penda Mboko River, suitability for drinking and irrigation use

50. Ngai, N. J., Wotany, E. R., Agyingi, C., & Nelson, M. A. (2024). Geological influence on groundwater quality in volcanic aquifers of Eastern Mount Cameroon, West of the Penda Mboko River. *Discover Applied Sciences*, 6(10), 541.

51. Ngwa, C. N., Lenhardt, N., Le Roux, P., & Mbassa, B. J. (2019). The Mount Cameroon southwest flank eruptions: Geochemical constraints on the subsurface magma plumbing system. *Journal of Volcanology and Geothermal Research, 384*, 179–188. https://doi.org/10.1016/j.jvolgeores.2019.07.001

52. Ngwese, S. N., Mouri, H., Akoachere II, R. A., McKinley, J., & Candeias, C. (2025). Potentially harmful elements in the geoenvironment: a status review of sources, impacts and regulatory framework in Cameroon, Central Africa. *Journal of African Earth Sciences*, 105728.

53. Njitchoua R, Sigha-Nkamdjou L. Dever L, Marlin C, Sighomnou D, Nia P., (1999) Variations of the stable isotopic compositions of rainfall events from the Cameroon rain forest, central Africa, J. Hydrol. 223, 17 – 26.

54. Nkotagu, H. (1996). The groundwater geochemistry in the semi-arid, fractured crystalline basement. Area of Dodoma, Tanzania. Journal of African Earth Science. 23(4), 593-505.

55. Nlend, B., Huneau, F., Ngo Boum-Nkot, S., Song, F., Komba, D., Gwodog, B., ... & Fongoh, E. (2023). Review of isotope hydrology investigations on aquifers of Cameroon (Central Africa): What information for the sustainable management of groundwater resources?. *Water*, *15*(23), 4056.

56. Oborie, H.O Nwankwoala (2014) Analysis of Major Ion Constituents in Groundwater of Amassoma and Environs, Bayelsa State, Nigeria Journal of Applied Chemistry, 2014, 2(5):1-13

57. Pederzani, S., & Britton, K. (2019). Oxygen isotopes in bioarchaeology: Principles and applications, challenges and opportunities. *Earth-Science Reviews*, *188*, 77-107.

58. Qu, S., Zhao, Y., Li, M., Zhang, K., Wang, J., Duan, L., ... & Yu, R. (2024). Spatio-seasonal characteristics and controlling factors of surface water stable isotope values (δ18O and δD) across the Inner Mongolia Reaches of the Yellow River Basin, China: Implication for hydrological cycle. *Journal of Hydrology: Regional Studies*, *53*, 101843.

59. Rozanski, K., Araguás-Araguás, L., & Gonfiantini, R. (1993). Isotope patterns in modern global precipitation. In P. K. Swart, K. C. Lohmann, J. McKenzie, & S. Savin (Eds.), Climate change in continental isotopic records (pp. 1–36). American Geophysical Union. https://doi.org/10.1029/GM078p0001

60. Saiers, J. E., Fair, J. H., Shanley, J. B., Hosen, J., Matt, S., Ryan, K. A., & Raymond, P. A. (2021). Evaluating streamwater dissolved organic carbon dynamics in context of variable flowpath contributions with a tracer-based mixing model. *Water Resources Research*, *57*(10), e2021WR030529.

61. Saka, D., Akiti, T.T., Osae, S., Appenteng, M.K., Abass, G. (2013). Hydrogeochemistry and isotope

studies of groundwater in the Ga West Municipal Area, Ghana. Appl Water Sci 3:577-588.

62. Scholl, M. A., Ingebritsen, S. E., Janik, C. J., & Kauahikaua, J. P. (1996). Use of precipitation and groundwater isotopes to interpret regional hydrology on a tropical volcanic island: Kilauea volcano area, Hawaii. *Water Resources Research*, *32*(12), 3525-3537.

63. Somers, L. D., & McKenzie, J. M. (2020). A review of groundwater in high mountain environments. *Wiley Interdisciplinary Reviews: Water*, *7*(6), e1475.

64. Taboada-Castro, M.M., Rodriquez-Blanco, M.L. (2012). Rainfall-runoff response and event-based runoff coefficients in a humid area (North west Spain). Hydrological sciences journal 57 (3), 445-459.

65. Takang, A. V., Wotany, E. R., & Christopher, A. (2025). Evaluation of surface water quality for domestic and agro-industrial applications along the tropical rainforest gradient, central Cameroon.

66. Terzer-Wassmuth, S., Araguás-Araguás, L. J., Wassenaar, L. I., & Stumpp, C. (2023). Global and local meteoric water lines for δ 17O/δ 18O and the spatiotemporal distribution of Δ′ 17O in Earth’s precipitation. *Scientific Reports*, *13*(1), 19056.

67. Todd D.K., Mays L.W. (2005). Groundwater Hydrology (3rd ed.). John wiley &Sons, Inc., United States of America.

68. Torres-Martínez, J. A., Mora, A., Knappett, P. S., Ornelas-Soto, N., & Mahlknecht, J. (2020). Tracking nitrate and sulfate sources in groundwater of an urbanized valley using a multi-tracer approach combined with a Bayesian isotope mixing model. *Water Research*, *182*, 115962.

69. US.EPA (2009). Statistical Analysis of Groundwater Monitoring Data at RCRA Facilities.

70. Vystavna, Y., Harjung, A., Monteiro, L. R., Matiatos, I., & Wassenaar, L. I. (2021). Stable isotopes in global lakes integrate catchment and climatic controls on evaporation. *Nature Communications*, *12*(1), 7224.

71. Wantim, M.N., Kervyn M., Ernest G.G.J., Jacobs P. (2013) Numerical Experiments on The Dynamics of Channelized Lava Flows at Mount Cameroon Volcano with The FLOWGO therrmo-rheological model. Journal of volcanology and Geothermal Research 253: 35-53.

72. Winter, T.C., Harvey, J.W., Franke O.L., Alley, W.M. (1998). Groundwater and surface water a single resource: U. S. Geological Survey Circular 1139.

73. Wirmvem, M.J., Ohba. T., Nche, L. A., Kamtchueng, B.T., Kongnso W.E., Mimba, E.M., Bafon G.T., Yaguchi, M., Eneke G.T., Fantong W.Y., Ako A.A. (2017). Effect of diffuse recharge and wastewater on groundwater contamination in Douala, Cameroon. Environ Earth Sci. p76:354 DOI 10.1007/s12665-017-6692-8.

74. Wotany E.R., Samuel N. Ayonghe, Wilson Y. Fantong, Mengnjo J. Wirmvem4 and Takeshi Ohba4 (2013) Hydrogeochemical and anthropogenic influence on the quality of water sources in the Rio del Rey Basin, South Western, Cameroon, Gulf of Guinea, 10.5897/AJEST2013.1578.

75. Wotany E.R., Wirmvem M.J, Fantong W.Y, Ayonghe S.N, Wantim M.N, Ohba T. (2021). Isotopic composition of precipitation and groundwater onshore of the Rio del Rey Basin, Southwest Cameroon: Local meteoric lines and recharge. Applied Water Science 19-0021

76. Zhang, P., Li, X., Yue, F. J., Zhang, Y., Wang, Y., Wu, D., ... & Ji, X. (2025). Anthropogenic nitrogen inputs favour increased nitrogen and organic carbon levels in Qinghai–Tibetan Plateau lakes: Evidence from sedimentary records. *Water Research*, *277*, 123330.

77. Zhu, G., Liu, Y., Wang, L., Sang, L., Zhao, K., Zhang, Z., ... & Qiu, D. (2023). The isotopes of precipitation have climate change signal in arid Central Asia. *Global and Planetary Change*, *225*, 104103.